Materials Science Forum
ISSN: 1662-9752, Vol. 910, pp 102-108
doi:10.4028/www.scientific.net/MSF.910.102

Submitted: 2017-02-02
Revised: 2017-04-17
Accepted: 2017-04-17
Online: 2018-01-03

Projectile Impact Testing Aluminum Corrugated Core Composite Sandwiches Using Aluminum Corrugated Projectiles: Experimental and Numerical Investigation

K. Odacı[1], C. Kılıçaslan[1], A. Taşdemirci[1], A.G. Mamalis[2] and M. Güden[1,a*]

[1]Dynamic Testing and Modeling Laboratory, Department of Mechanical Engineering, Izmir Institute of Technology, Izmir, Turkey

[2]Project Center for Nanotechnology and Advanced Engineering, NCSR “Demokritos”, Athens, Greece

[a]mustafaguden@iyte.edu.tr

Keywords: Corrugated core; composite plate; direct impact; numerical simulation

Abstract. E-glass/polyester composite plates and 1050 H14 aluminum trapezoidal corrugated core composite sandwich plates were projectile impact tested using 1050 H14 aluminum trapezoidal fin corrugated projectiles with and without face sheets. The projectile impact tests were simulated in LS-DYNA. The MAT_162 material model parameters of the composite were determined and then optimized by the quasi-static and high strain rate tests. Non-centered projectile impact test models were validated by the experimental and numerical back face displacements of the impacted plates. Then, the centered projectile impact test models were developed and the resultant plate displacements were compared with those of the TNT mass equal Conwep simulations. The projectiles with face sheets induced similar displacement with the Conwep blast simulation, while the projectiles without face sheets underestimated the Conwep displacements, which was attributed to more uniform pressure distribution with the use of the face sheets on the test plates.

Introduction

Closed-cell aluminum foam projectiles are widely used to investigate to impose blast-like pressure-time profile on the targets [1-8]. However, the dispersion in the strength of aluminum closed-cell foams, is in the order of 20% [1]. The corrugated layered structures such as trapezoidal corrugated aluminum [9, 10], on the other side, are homogenous in structure and display repeatable mechanical properties. Mainly motivated for above, in this study, a 1050 H14 Al trapezoidal corrugated aluminum layered structure was used as the projectile to test E-glass/Polyester composite plates and corrugated core composite sandwiches. The composite material model parameters were determined and then optimized by the quasi-static and high strain rate tests. The composite plates of three different thicknesses and the composite face sheet-single and 3-fin layer corrugated core sandwiches were projectile impact tested using cylindrical corrugated projectiles. The quasi-static, dynamic and projectile impact tests of the composite and composite sandwiches were simulated in the explicit finite element code of LS-DYNA. The experimentally and numerically determined back face displacements of the composite and sandwich plates were compared with the displacements of the Conwep blast simulations in LS-DYNA. The results have shown that the used corrugated structure can generate shock loading as similar with explosive blast loading and can be used to produce shock-like loads in laboratory scale experiments.

Experimental and Modelling

E-glass/polyester composite plates were prepared by the resin transfer molding using a Metyx biaxial E-glass fabric (954 g m^{-2}) and a Scott Bader Crystic 703 PA polyester resin. The composite plates were prepared in 2, 5 and 8 mm thicknesses, while 2 mm-thick composite plates were used as the face sheet in the composite sandwich plates. The height, width, length and thickness of a fin layer in the projectile were sequentially 3, 1.5, 2.5 and 0.135 mm. The fin layer for the sandwiches were made from the same Al alloy as the projectile but with the height, width, length and thickness of 9, 0.75, 1.5 and 0.135 mm, respectively. The composite face sheet corrugated core sandwich panels were assembled using a polyurethane adhesive (Henkel Thomsit R710). The sandwich panels were kept under 5 kg loads for 2 h in order to satisfy full sticking between composite face sheets and cores. The composite sandwich samples were prepared using the single and 3-fin layers (Figs. 1(a) and (b)). In three-fin layer core composite sandwich, Al 1050 H14 interlayer sheets in 0.5 mm thickness were inserted between each corrugated fin layer, while there was no interlayer sheets in single-fin layer core sandwich structure. The single-fin layer core sandwich had the same areal density with 5 mm-thick composite plate, while 3-fin layer core sandwich with 8 mm-thick composite plate. The projectile impact tests were conducted on the composite and sandwich plates using a gas gun test set-up. The details of the gas gun test set-up used is given in ref. [11]. The projectile impact velocities were measured with the laser barriers in the front and back of the specimen holder frames and the impact test was recorded with a high speed camera (20000 fps). The displacements of the tested plates were determined both from the camera records and the tested specimen before removed from the test frame. The composite was modeled using MAT_162 material model in LS-DYNA PrePost software. The principle directions of X, Y and Z are represented as a, b and c in the material model, respectively. The MAT_162 combines the composite failure developed by Hashin [12] with the damage developed by Matzenmiller [13] and the strain softening after failure. Several examples of the MAT_162 material model parameter prediction of fiber reinforced composites are found in the literature, refs. [14-16]. It predicts the fiber fill tensile/shear failure, fiber warp tensile/shear failure, in-plane compressive failure in fiber fill and warp directions, the crush failure under compression and in-plane and through-thickness matrix failure modes. The damage functions are derived from the fiber and matrix failure modes by ignoring the Poisson's effect. Elastic moduli reduction is expressed in terms of the damage parameter $\overline{w}_i$ as [17]

$$E_i' = (1 - e^{-\frac{r_i^{m_i}}{m_i}})E_i \quad r_i > 0, i = 1, \ldots 6 \tag{1}$$

where, E_i is the initial elastic modulus, E_i' is the reduced elastic modulus, r_i is the damage threshold computed from the associated damage functions for fiber and matrix damage and delamination and m_i is the material damage parameter. The damage function is formulated to account for the overall nonlinear elastic response of a lamina including the initial hardening and subsequent softening beyond the ultimate strength. Four damage parameters of m are used for the post elastic damage response under different loading conditions. AM_1 is for the fiber damage in the X direction, AM_2 is the fiber damage in the Y direction, AM_3 is the fiber crush and punch shear damage and AM_4 is the matrix failure and delamination. Strain rate sensitivities in terms of the strength properties (S) and elastic moduli are formulated as [17]

$$\{S_{rt}\} = \{S_0\}\left(1 + C_{rate1}\ ln\frac{\dot{\bar{\varepsilon}}}{\dot{\varepsilon_0}}\right) \tag{2}$$

$$\{\mathrm{E_{rt}}\} = \{\mathrm{E_0}\}\left(1 + \{\mathrm{C_{rate}}\}\ \ln\frac{\dot{\bar{\varepsilon}}}{\dot{\varepsilon_0}}\right) \tag{3}$$

where, $\dot{\bar{\varepsilon}}$ and $\dot{\varepsilon_0}$ are the equivalent strain rate and reference strain rate, respectively, C_{rate} is the strain rate parameter; C_1 is the strain rate constant for strength properties, C_2 for the elastic moduli in the X direction, C_3 for the shear moduli and C_4 for the elastic moduli in the Z direction. The tests and numerical models used to determine and optimize the MAT_162 material model parameters of the tested composite are given elsewhere [18]. The numerical model of the projectile impact testing of the composite sandwich plates with single and 3-fin layer corrugated core are shown in Figs. 2(a) and (b), respectively. The models consist of top and bottom frames, projectile and composite sandwich specimen. The frames used to fix the plates in the projectile impact test were considered to be rigid and each frame compromised of 11232 solid elements. The sandwich panel with 3-fin layer corrugated core was modelled using 343488 shell, 116236 constant solid stress and 22464 rigid elements. The single-fin layer corrugated core composite sandwich plate was modelled using 239808 shell, 87116 constant solid stress and 22464 rigid elements.

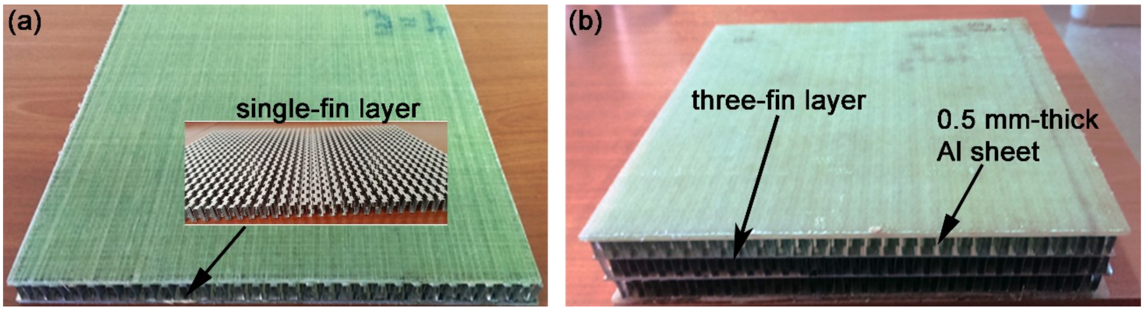

Fig. 1. Corrugated core composite sandwich plates with (a) single and (b) 3-fin layer cores.

Results and Discussion

The optimized MAT_162 material model parameters of the composite are tabulated in Table 1. Based on the type of the experiments, the damage parameters AM, ELIMT, EEXPN and SDELM can be calibrated. The deformation of the projectile intensified as the thickness of the plate increased and the corrugated projectile was fully densified when 8 mm-thick composite plate was tested. The experimental and numerical delamination pictures of 5 and 8 mm-thick composite plates are shown sequentially in Figs. 3(a-d). The delamination area was calculated approximately by drawing the rectangles covering the delamination zone on the pictures of the tested plates. In 2 mm-thick composite plate, the experimental and numerical delamination areas were sequentially 26505 and 26243 mm^2; the discrepancy was ~1%. In 5 mm-thick composite plates, the experimental (Fig. 3(a)) and numerical (Fig. 3(b)) delamination areas are sequentially 22436 and 21880 mm^2, with a discrepancy of ~2.48%. In 8 mm-thick composite plates, the experimental (Fig. 3(c)) and numerical (Fig. 3(d)) delamination areas are 21390 and 20727 mm^2, respectively and the discrepancy is ~3.1%. The experimental and numerical maximum displacements of the composites tested with and without face sheets are tabulated in Table 2. The projectile impact locations on the composite plates in the numerical models were the same as the experiments. The numerical displacements show well agreements with the experimental displacements with a maximum error of 17.45%. The delamination areas of single-fin layer sandwich were sequentially 18200 and 19044 mm^2, with a discrepancy of ~4.64%. The delamination zone in the back face sheet was found smaller than the delamination zone in the front face. The corrugated projectile used was experimentally and numerically crushed up to 0.81 and 0.79 strain, respectively. The maximum displacement was 9.58 mm at the impact zone. The experimental and numerical front face delamination pictures of 3-fin layer core sandwich are shown in Figs. 4(a-d). The experimental (Fig. 4(a)) and numerical (Fig. 4(b)) delamination areas are 16380 and 17526 mm^2, respectively, with a discrepancy of ~6.99%. There is no back face sheet delamination in experimentally and numerically tested 3-fin layer core sandwiches (Figs. 4(c) and (d)). The experimental and numerical side views of the 3-fin layer core sandwich after the test show very much similarities as shown in Figs. 4(e) and (f), respectively. The maximum displacement is 8.84 mm at the impact zone. The numerical center-impacted maximum back face displacements of the composite and sandwich plates tested with without and with face sheet projectiles are shown in Figs. 5(a) and (b), respectively. As is expected 2 mm-thick composite has the highest displacement at all impact velocities. On the other side, 5 mm-thick composite plate and its mass equivalent single-fin layer corrugated core sandwich plate show similar displacements up to 50-60 m s^{-1}, while the sandwich exhibits 45.93% lower back face displacement than the composite counterpart at 200 m s^{-1}. Similarly, 8 mm-thick composite plate and its mass equivalent 3-fin layer corrugated core sandwich have similar displacements up to 100 m s^{-1}. The sandwich structure however shows 37.92% lower back face displacement than the composite counterpart at 200 m s^{-1}. The center-impacted plate displacements were then compared with the displacements of the equivalent Conwep blast loading of the plates. The equivalent TNT mass with a 0.5 m stand-off distance was calculated for each impact velocity from direct impact SHPB simulations at the same impact velocity. Based on this, the equivalent TNT masses were found 0.02, 0.035, 0.06, 0.105, 0.235 and 0.4 kg for the impact velocity of 25, 50, 75, 100, 150 and 200 m s^{-1}, respectively (Fig. 5(c)). A parabolic fit to the TNT mass-velocity data in Fig. 5(c) gives the TNT mass equivalent-velocity relation up to 200 m s^{-1}.

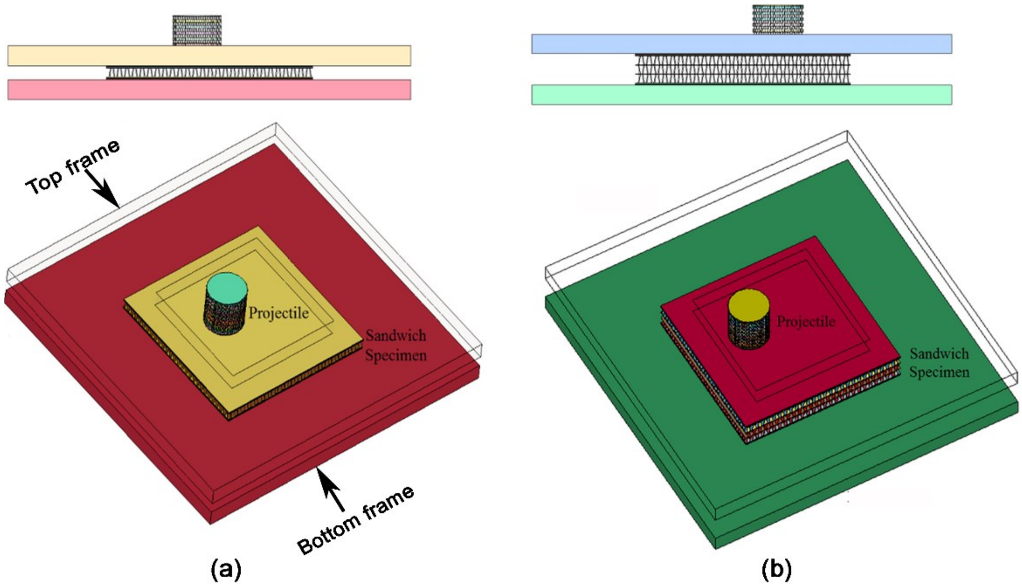

Fig. 2. Projectile impact test model of the sandwich panels with (a) single and (b) 3-fin layer corrugated core.

Table 1. Optimized MAT_162 material model parameters.

Parameter	Value	Parameter	Value	Parameter	Value	Parameter	Value
$\rho, kg/m^3$	1850	G_{31}, GPa	1.66	S_{FC}, MPa	650	$C_{rate\,1}$	0.033
E_1, GPa	16	S_{12}, MPa	43.4	S_{FS}, MPa	325	*AM 1*	4
E_2, GPa	16	S_{23}, MPa	43.4	S_{FFC}	0.3	*AM 2*	4
E_3, GPa	7.74	S_{31}, MPa	43.4	φ, deg	10	*AM 3*	0.5
v_{21}	0.13	S_1^T, MPa	400	e_{Limit}	4	*AM 4*	2
v_{31}	0.23	S_1^C, MPa	285	S_{Delam}	1.2	C_{rate2}	0.036
v_{32}	0.23	S_2^T, MPa	400	ω_{max}	0.999	$C_{rate\,3}$	0.03
G_{12}, GPa	1.79	S_2^C, MPa	285	e_{Crush}	0.55	$C_{rate\,4}$	0.042
G_{23}, GPa	1.66	S_3^T, MPa	30	e_{Expn}	4		

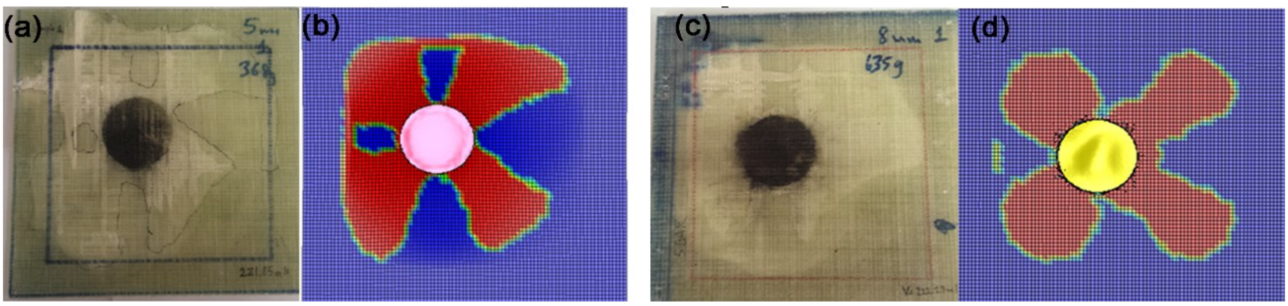

Fig. 3. Delamination zones in: 5 mm-thick composite (a) experimental, (b) numerical and 8 mm–thick composite (c) experimental and (d) numerical.

Table 2. Numerical and experimental displacements of the composite plates.

Specimen	Projectile	Velocity (m/s)	Experimental Displacement (mm)	Numerical Displacement (mm)	Error (%)
2 mm	With face sheet	222-231	45-48	46.34-51.84	2.9-8
5 mm		196.27-221.85	19-21.5	17.18-21.29	9.6-1
8 mm		197.24-222.23	8.5-12.4	8.6250-11.820	1.6-4.7
2 mm	Without face sheet	222-231	31-34	31.99-35.712	3.2-5
5 mm		196.27-221.85	12.5-14.9	11.904-12.30	4.8-17.4
8 mm		197.24-222.23	6.2-9.8	5.721-8.258	7.7-15.7

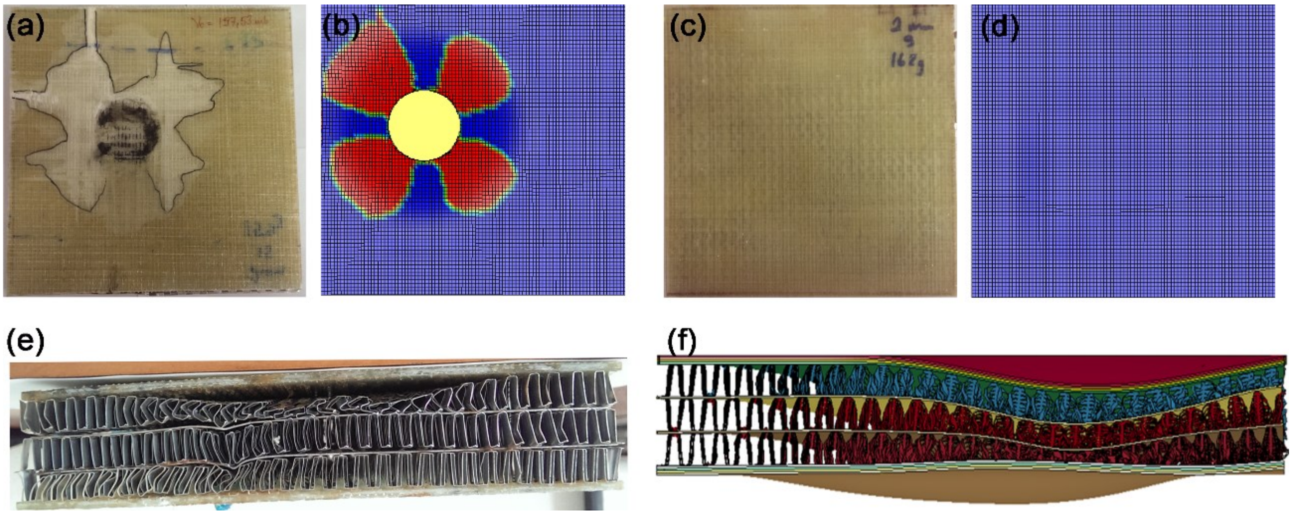

Fig. 4. Delamination regions in 3-fin layer core sandwich front face (a) experimental and (b) numerical and back face (c) experimental and (d) numerical and the side views of the impacted sandwich (e) experimental and (f) numerical.

The displacements of 2, 5 and 8 mm-thick composite plates impacted with the projectiles with face sheets and the corresponding displacements of the Conwep simulation are shown together in Fig. 6(a). It was found that the projectiles with face sheets showed a better agreement with blast simulations than the projectiles without face sheets. The face sheets in the simulation behave like an interface and distribute the load to the target more uniformly. The displacements of sandwich panels with single and 3-fin layer sandwiches tested without and with face sheet projectiles and Conwep blast simulations are shown in Figs. 6(b) and (c). Two types of the Conwep blast simulations are implemented in this figure: the TNT mass-equivalent determined from the direct impact tests and from the projectile impact simulations at the contact region on the sandwich plate. It is noted that the pressure developed on the composite is reduced when the TNT mass-equivalent determined from the direct impact tests. Based on this, TNT mass equivalent is modified and the resultant displacements are shown in Fig. 5(c) as function impact velocity. The maximum discrepancy between the projectile impact and Conwep simulations is reduced to 17.1% and 8.09% by modifying the TNT masses for single and 3-fin layer corrugated core sandwich structures, respectively (Figs. 6(b) and (c)). It is also noted that the projectiles without face sheets impose lower displacements compared to the projectiles with face sheet due to the lower kinetic energy. The projectile impact and Conwep blast simulation pictures of 8 mm composite plate and single and 3-fin layer sandwich plates at 100 m s^{-1} are shown in Fig 7. The projectile impact simulations show well agreements with the Conwep blast simulations. In projectile test, the pressure effected zone on the 8-mm thick plate is smaller than that of the Conwep simulation because the entire face of the plate is selected as the target in the Conwep simulations. This discrepancy changes the deformation profile of the back face while the maximum displacements are still very close to each other. The same discrepancy can also be seen in the sandwich panels.

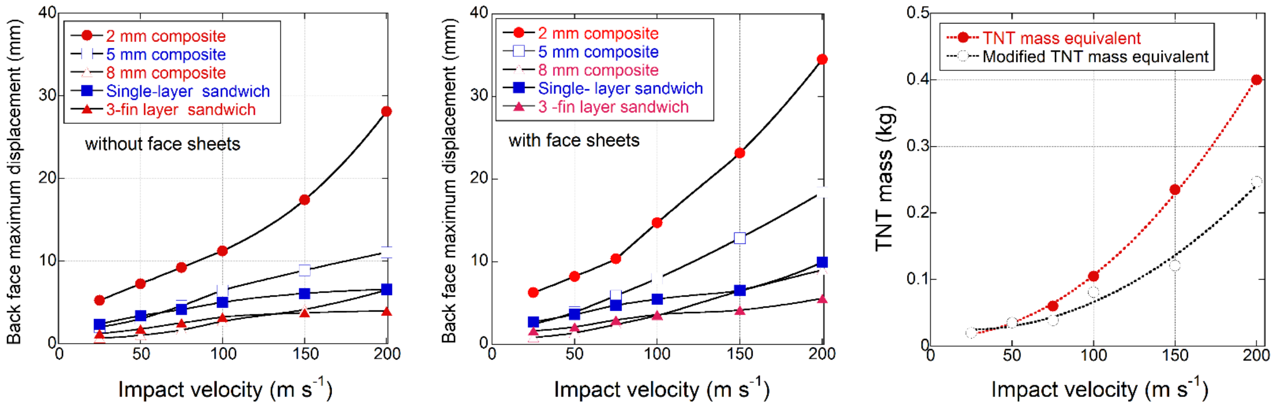

(a) (b) (c)

Fig. 5. Back face maximum displacements of the composite and sandwich plates impacted by the projectile with (a) without and (b) with face sheets and (c) TNT mass equivalent vs. impact velocity.

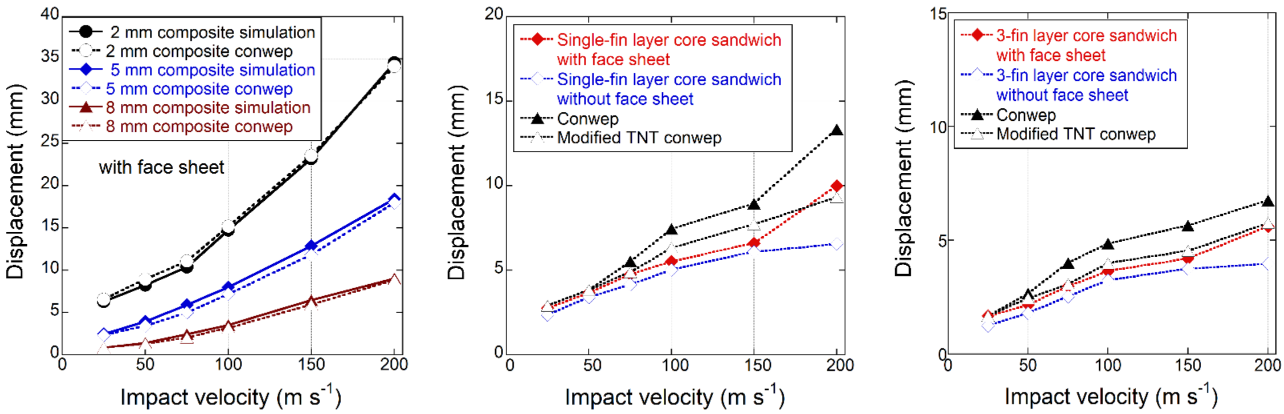

(a) (b) (c)

Fig. 6. (a) projectile impact and Conwep back face displacements of the composites with face sheet projectiles and projectile impact, Conwep and modified Conwep back face displacement of (b) single and (c) 3-fin layer composite sandwiches tested with and without face sheet projectiles.

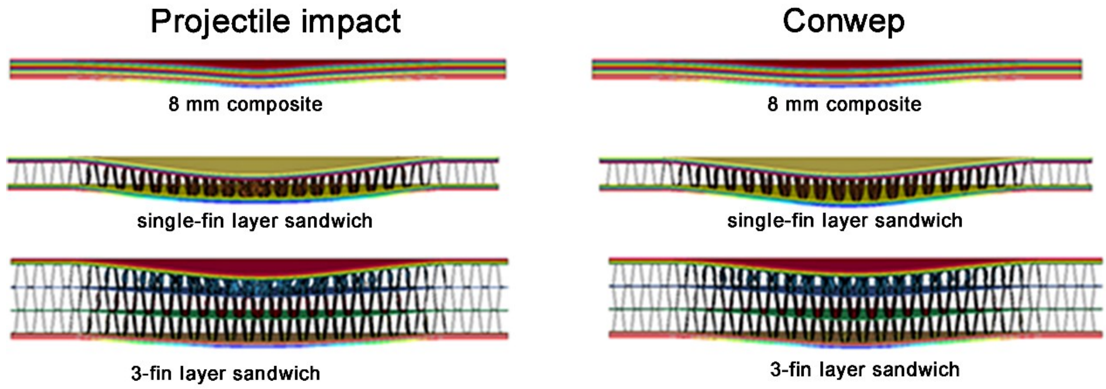

Fig. 7. The numerical deformation pictures of the composite and sandwich plates tested with the projectiles with face sheets at 100 m s^{-1} and the corresponding modified mass-equivalent TNT blast simulation pictures.

Conclusions

A non-explosive blast-like testing method was investigated by firing 1050 H14 aluminum trapezoidal fin corrugated core sandwich projectiles without and with face sheets to E-glass/polyester composite plates and corrugated core composite sandwich plates. The projectile impact tests of the composite and composite sandwich plates were simulated in LS-DYNA. The composite was modelled using MAT_162 material model. The experimental and numerical results were then compared with the Conwep blast simulations to validate the non-explosive blast-like testing method. The projectiles with face sheets showed better agreements with the Conwep blast simulation, while the projectiles without face sheets underestimated the Conwep displacements. This study showed that the corrugated core sandwich structures can generate shock loading as in the explosive blast.

References

[1] V.S. Deshpande, N.A. Fleck, High strain rate compressive behaviour of aluminium alloy foams, International Journal of Impact Engineering, 24 (2000) 277-298.

[2] S.L. Lopatnikov, B.A. Gama, M.J. Haque, C. Krauthauser, J.W. Gillespie, M. Guden, I.W. Hall, Dynamics of metal foam deformation during Taylor cylinder-Hopkinson bar impact experiment, Composite Structures, 61 (2003) 61-71.

[3] D.D. Radford, V.S. Deshpande, N.A. Fleck, The use of metal foam projectiles to simulate shock loading on a structure, International Journal of Impact Engineering, 31 (2005) 1152-1171.

[4] P.J. Tan, S.R. Reid, J.J. Harrigan, Z. Zou, S. Li, Dynamic compressive strength properties of aluminium foams. Part II - 'shock' theory and comparison with experimental data and numerical models, J. Mech. Phys. Solids, 53 (2005) 2206-2230.

[5] I. Elnasri, S. Pattofatto, H. Zhao, H. Tsitsiris, F. Hild, Y. Girard, Shock enhancement of cellular structures under impact loading: Part I experiments, J. Mech. Phys. Solids, 55 (2007) 2652-2671.

[6] R.P. Merrett, G.S. Langdon, M.D. Theobald, The blast and impact loading of aluminium foam, Materials & Design, 44 (2013) 311-319.

[7] H. Liu, Z.K. Cao, G.C. Yao, H.J. Luo, G.Y. Zu, Performance of aluminum foam–steel panel sandwich composites subjected to blast loading, Materials & Design, 47 (2013) 483-488.

[8] M. Peroni, G. Solomos, V. Pizzinato, Impact behaviour testing of aluminium foam, International Journal of Impact Engineering, 53 (2013) 74-83.

[9] C. Kilicaslan, M. Guden, I.K. Odaci, A. Tasdemirci, The impact responses and the finite element modeling of layered trapezoidal corrugated aluminum core and aluminum sheet interlayer sandwich structures, Materials & Design, 46 (2013) 121-133.

[10] C. Kilicaslan, M. Guden, I.K. Odaci, A. Tasdemirci, Experimental and numerical studies on the quasi-static and dynamic crushing responses of multi-layer trapezoidal aluminum corrugated sandwiches, Thin-Walled Structures, 78 (2014) 70-78.

[11] I.K. Odaci, C. Kilicaslan, A. Tasdemirci, M. Guden, Projectile impact testing of glass fiber-reinforced composite and layered corrugated aluminium and aluminium foam core sandwich panels: a comparative study, International Journal of Crashworthiness, 17 (2012) 508-518.

[12] Z. Hashin, Failure Criteria for Unidirectional Fiber Composites, Journal of Applied Mechanics, 47 (1980) 329-334.

[13] A. Matzenmiller, J. Lubliner, R.L. Taylor, A constitutive model for anisotropic damage in fiber-composites, Mechanics of Materials, 20 (1995) 125-152.

[14] A. Tasdemirci, A. Kara, A.K. Turan, G. Tunusoglu, M. Guden, I.W. Hall, Experimental and Numerical Investigation of High Strain Rate Mechanical Behavior of a [0/45/90/ - 45] Quadriaxial E-Glass/Polyester Composite, Procedia Engineering, 10 (2011) 3068-3073.

[15] L.J. Deka, S.D. Bartus, U.K. Vaidya, Damage evolution and energy absorption of E-glass/polypropylene laminates subjected to ballistic impact, J Mater Sci, 43 (2008) 4399-4410.

[16] J.R. Xiao, B.A. Gama, J.W. Gillespie Jr, Progressive damage and delamination in plain weave S-2 glass/SC-15 composites under quasi-static punch-shear loading, Composite Structures, 78 (2007) 182-196.

[17] LSTC, LS-DYNA Keyword User's Manual vol. II: Livermore Software Technology Corporation (LSTC), in, 2007.

[18] K. Odacı, Experimental and numerical evaluation of the blast-like loading of fiber reinforced polymer composites and aluminum corrugated core composite sandwiches through projectile impact testing using aluminum corrugated projectiles, PhD thesis Mechanical Engineering, İzmir Institute of Technology, İzmir, Turkey, 2015.